

## INFLUENCE OF TIME AND TEMPERATURE IN THE MICROWAVE-ASSISTED HYDROTHERMAL TREATMENT OF MAGNETITE NANOPARTICLES

Cristina CHIRCOV<sup>1</sup>, Raluca Elena ȘTEFAN<sup>2</sup>, Anton FICAI<sup>3</sup>,  
Ecaterina ANDRONESCU<sup>4</sup>

**Abstract.** Magnetite is an iron oxide that has been extensively investigated for its utilization in the development of drug delivery nanocarriers. Generally, magnetite nanoparticles are obtained through the chemical route of co-precipitation. However, since the outcome properties of the resulted nanoparticles are limited in terms of possibility to control the size and size distribution and to ensure the reproducibility of the synthesis process, unconventional synthesis routes are constantly investigated. Specifically, the microwave-assisted hydrothermal method represents an alternative with tremendous potential owing to the possibility of varying the treatment parameters, i.e., pressure, temperature, time. Thus, the present study aimed to investigate the influence of time and temperature upon the structural and physico-chemical properties of magnetite nanoparticles.

**Keywords:** magnetite nanoparticles, microwave-assisted hydrothermal method, drug delivery  
DOI <https://doi.org/10.56082/annalsarsciphyschem.2023.2.19>

### 1. Introduction

Iron oxides represent transition metal oxides that occur naturally in numerous polymorphs with varying stoichiometries and structures and have important roles in numerous geological and biological processes [1, 2]. Additionally, iron oxide nanoparticles possess unique properties, such as superparamagnetic behavior, high saturation magnetization, good dispensability, and biocompatibility [3]. Among them, magnetite ( $\text{Fe}_3\text{O}_4$  or  $\text{FeO}\cdot\text{Fe}_2\text{O}_3$ ) is one of the most intensively studied and applied forms owing to its unique magnetic properties that are of significant importance in medical and technological applications, such as such as separation

---

<sup>1</sup>Teaching Assistant, Department of Science and Engineering of Oxide Materials and Nanomaterials, National University of Science and Technology Politehnica Bucharest, Bucharest, Romania, [cristina.chircov@yahoo.com](mailto:cristina.chircov@yahoo.com).

<sup>2</sup>Eng, Department of Science and Engineering of Oxide Materials and Nanomaterials, National University of Science and Technology Politehnica Bucharest, Bucharest, Romania, [ralucastefan98@yahoo.com](mailto:ralucastefan98@yahoo.com).

<sup>3</sup>Prof., PhD, Department of Science and Engineering of Oxide Materials and Nanomaterials, National University of Science and Technology Politehnica Bucharest, Bucharest, Romania, full member of the Romanian Academy, [anton.ficai@upb.ro](mailto:anton.ficai@upb.ro).

<sup>4</sup>Prof., PhD, Department of Science and Engineering of Oxide Materials and Nanomaterials, National University of Science and Technology Politehnica Bucharest, Bucharest, Romania, full member of the Romanian Academy, [ecaterina.andronescu@upb.ro](mailto:ecaterina.andronescu@upb.ro).

---

and purification, drug delivery, localized therapeutic hyperthermia, biosensing, or as contrast agents in magnetic resonance imaging [4-6].

In terms of crystalline properties, the mineralogical structure of magnetite involves a spinel cubic crystal system (Fd3m space group) [4-8], with the face-centered cubic lattice formed by the oxygen ions where the iron(II) ions are occupy half of the octahedral sites, while the iron(III) ions are distributed within the tetrahedral sites and the other half of the octahedral sites [4-6]. Generally, the size of magnetite nanoparticles can range between 5 and 100 nm, among which the nanoparticles with sizes below 25 nm exhibit superparamagnetic behavior. In regard to shape, magnetite nanoparticles are most commonly spherical [9, 10].

Magnetite nanoparticles can be obtained through a variety of methods that can be divided into chemical, physical, and biological methods. Owing to its rapidness, simplicity, and cost-effectiveness, the chemical route of co-precipitation remains one of the most commonly applied techniques [11], which involves the co-precipitation of iron(II) and iron(III) precursors at a 1:2 molar ratio in an alkaline medium in the form of hydroxides and the subsequent formation of the mixed iron oxide [12, 13]. However, the co-precipitation technique is characterized by several disadvantages that constrain its suitability for developing drug delivery systems based on magnetite nanocarriers, such as broad nanoparticle size distributions and limited batch-to-batch reproducibility [6, 14].

Therefore, unconventional synthesis methods are constantly investigated for overcoming the limitations of the co-precipitation method. Among them, the microwave-assisted hydrothermal synthesis represents a promising alternative. In this case, the precursor solutions are exposed to a sealed container, under high temperature and pressure conditions [15-18], which lead to a high degree of crystallinity and well-defined morphology and size [19-21]. Furthermore, the microwave-assisted hydrothermal method allows for a highly homogenous internal heating that rapidly rises the temperature by avoiding heat conduction due to the excitation produced by the interactions of the microwave electromagnetic radiations and the material [1, 22-26].

In this manner, the present study aimed to investigate the influence of the parameters involved in the microwave-assisted hydrothermal process, i.e., treatment time and temperature, upon the structural and physico-chemical properties of magnetite nanoparticles.

## **2. Materials and methods**

Ferric chloride hexahydrate ( $\text{FeCl}_3 \cdot 6\text{H}_2\text{O}$ ), ferrous sulfate heptahydrate ( $\text{FeSO}_4 \cdot 7\text{H}_2\text{O}$ ), and ammonium hydroxide 25% ( $\text{NH}_4\text{OH}$ ) were purchased from

---

Sigma-Aldrich Merck (Darmstadt, Germany) and they were used with no further purification.

The magnetite nanoparticles were synthesized through the microwave-assisted hydrothermal method based on a procedure described in our previous studies [27, 28]. Briefly, the precursors were dissolved in ultrapure water (at a molar ratio  $\text{FeCl}_3 \cdot 6\text{H}_2\text{O}:\text{FeSO}_4 \cdot 7\text{H}_2\text{O}$  of 1:2) and further dripped into the alkaline  $\text{NH}_4\text{OH}$  solution through a peristaltic pump. The obtained mixture was transferred into a Teflon vessel that was subjected to the microwave-assisted hydrothermal treatment using the Milestone Synthwave equipment. Table 1 summarizes the six different parameter regimes that led to the obtaining of six different samples. After naturally cooling to room temperature, the nanoparticles were decanted with a high-power magnet, washed several times with ultrapure water until the pH was neutral, and dried overnight at 60 °C.

**Table 2.** The parameter regimes used for obtaining the magnetite nanoparticles through the microwave-assisted hydrothermal method.

<i>Sample code</i>	<i>Pressure [bar]</i>	<i>Temperature [°C]</i>	<i>Time [min]</i>
3-30-15	3	30	15
3-30-30			30
3-30-60			60
3-60-15		60	15
3-60-30			30
3-60-60			60

The magnetite nanoparticles were further characterized through X-ray diffraction (XRD) in order to assess the mineralogical phases present within the samples. The measurements were performed between the  $2\theta$  angles of 10 and 80° using a  $\text{CuK}\alpha$  radiation source within a PANalytical Empyrean diffractometer (PANalytical, Almelo, The Netherlands). Subsequently, the obtained diffractograms were subjected to the Rietveld refinement algorithm for calculating the unit cell parameters, the average crystallite size, and the crystallinity of the nanoparticles.

Furthermore, the samples were evaluated through dynamic light scattering in order to assess the hydrodynamic diameter and polydispersity index and zeta potential measurements for investigating their stability in aqueous media. The measurements were performed in triplicate in ultrapure water with a pH of 6.9, using a DelsaMax Pro equipment.

### 3. Results and discussion

The obtained magnetite nanoparticles were evaluated in regard to the influence of time and temperature of the microwave-assisted hydrothermal treatment upon their structural and physico-chemical properties.

In this manner, Fig. 1 depicts the diffractograms acquired for the 3-30-15, 3-30-30, 3-30-60, 3-60-15, 3-60-30, and 3-60-60 samples, respectively. As the diffractograms show through the characteristic Miller indices (JCPDS 00-019-0629 [29, 30]), all samples contain magnetite as the unique mineralogical phase in the cubic crystallization system with the  $Fd3m$  space group. By contrast to our previous study, the parameter regimes used in the current study did not lead to the formation of secondary phases, e.g., goethite [27].

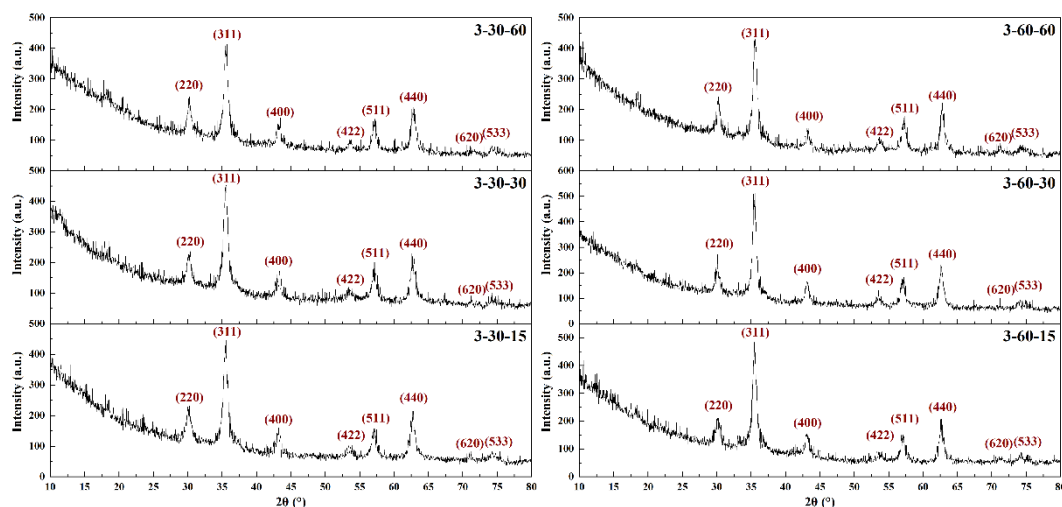


**Fig. 2.** Diffractograms acquired for the 3-30-15, 3-30-30, 3-30-60, 3-60-15, 3-60-30, and 3-60-60 samples.

Moreover, the acquired diffractograms were fitted using the Rietveld refinement algorithm in order to determine the unit cell parameters, the average crystallite size, and the crystallinity of the samples (Table 2). As the results show, when applying a temperature of 30 °C, increasing the time of the microwave-assisted hydrothermal treatment leads to a proportional increase of the average crystallite size due to the particle growth processes that occur. However, the crystallinity of the samples increases up to the time of 30 min, followed by a significant decrease. Thus, longer treatment times lead to the formation of an amorphous phase. A similar behavior was observed for the samples obtained at the temperature of 60 °C, with values higher than the samples obtained at a lower temperature. In regard to the average crystallite size, the variation is proportional to the crystallinity values, as it increases up to the time of 30 min, followed by a significant decrease for the time of 60 min.

**Table 3.** The parameter regimes used for obtaining the magnetite nanoparticles through the microwave-assisted hydrothermal method.

Sample	Unit cell parameters		Average Crystallite Size [nm]	Crystallinity [%]
	$a = b = c$ [Å]	$\alpha = \beta = \gamma$ [°]		

3-30-15	8.369	90	8.23	18.61
3-30-30	8.360	90	8.45	19.02
3-30-60	8.363	90	10.78	15.85
3-60-15	8.369	90	9.09	19.92
3-60-30	8.373	90	10.03	20.00
3-60-60	8.364	90	9.81	17.74

Furthermore, the hydrodynamic diameter and the polydispersity index of the obtained magnetite nanoparticles was evaluated through dynamic light scattering (Fig. 2). As it can be observed, when applying a lower temperature of the microwave-assisted hydrothermal treatment, the hydrodynamic diameter and the polydispersity index decrease with the time, which demonstrates that longer treatments lead to the obtaining of more monodisperse nanoparticles. This observation is in accordance with the size distribution graphs depicted in Fig. 3. By contrast, when applying the temperature of 60 °C, the polydispersity index increases with the treatment time, as also shown in the size distribution graphs. However, in this case, the lowest hydrodynamic diameter value was registered for the 3-60-30 sample, which could be associated with a lower agglomeration tendency.

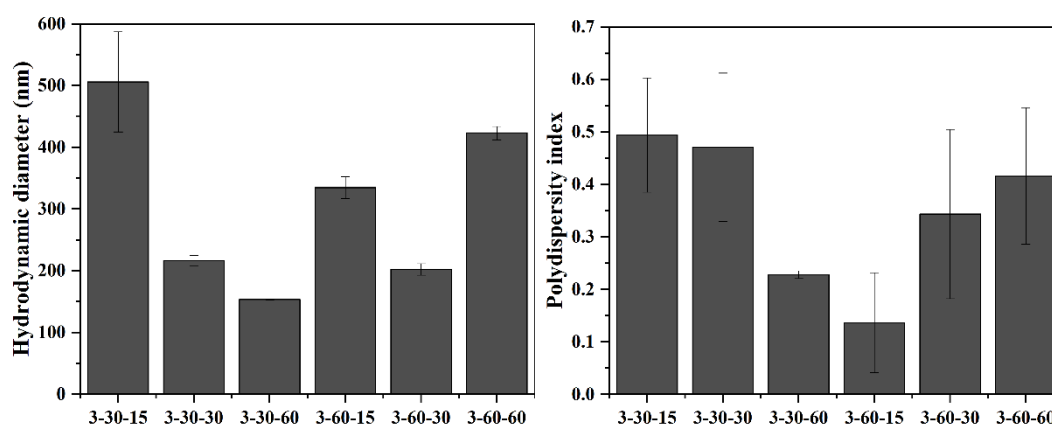


**Fig. 3.** Hydrodynamic diameter (left) and polydispersity index (right) values for the for the 3-30-15, 3-30-30, 3-30-60, 3-60-15, 3-60-30, and 3-60-60 samples.

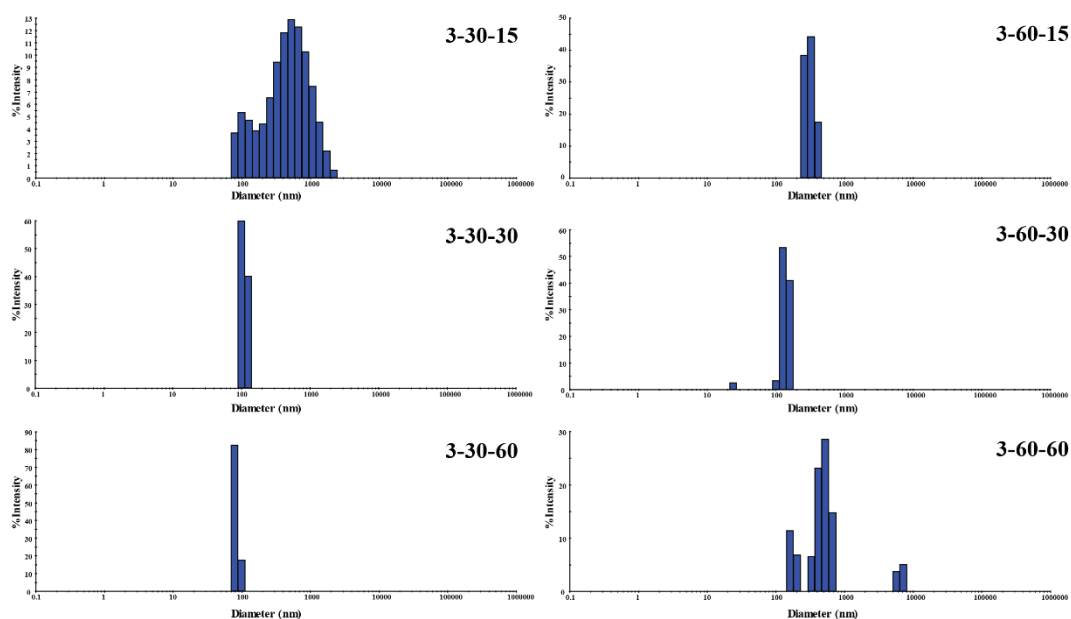


**Fig. 4.** values for the for the 3-30-15, 3-30-30, 3-30-60, 3-60-15, 3-60-30, and 3-60-60 samples.

The previously mentioned observations were further confirmed by the zeta potential measurements (Fig. 4). Samples 3-30-15, 3-30-30, and 3-60-30 exhibit zeta potential values higher than 25 mV, which is generally associated with an increased electrostatic stability and low agglomeration tendency when dispersed into fluid media [31].

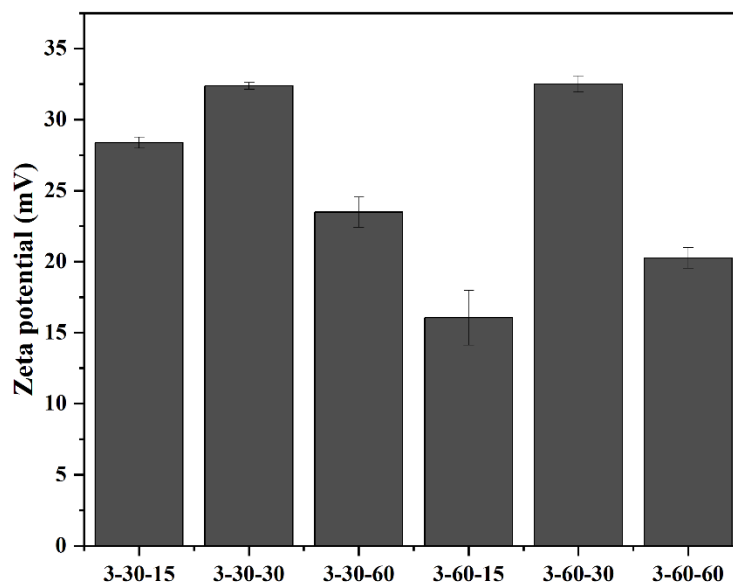


**Fig. 5.** Zeta potential values for the for the 3-30-15, 3-30-30, 3-30-60, 3-60-15, 3-60-30, and 3-60-60 samples.

Therefore, based on the obtained results, it could be safe to assume that the optimal results regarding nanoparticle crystallinity, size distribution, and electrostatic stability were obtained for the sample obtained in the 3 bar, 60 °C, and 30 min parameter regime.

## Conclusions

Although it is the most widely applied synthesis procedure for the obtaining of magnetite nanoparticles, the co-precipitation method is characterized by a series of disadvantages in regard to broad nanoparticle size distributions and limited batch-to-batch reproducibility. Therefore, novel and unconventional synthesis techniques are constantly being investigated for their potential to outcome such limitations. In the current study, the microwave-assisted hydrothermal method was employed for the obtaining of magnetite nanoparticles at six different parameter regimes involving pressure, temperature, and time.

Based on the obtained results, it was concluded that higher temperatures lead to increased crystallinity of the nanoparticles with narrower size distributions and increased dispersion stability.

However, longer time treatments, i.e., 60 min, lead to a decrease in both nanoparticle crystallinity and zeta potential values.

Thus, the optimal results were obtained for the sample obtained at 3 bar, 60 °C, and 30 min, which could be further used in the development of magnetite-based drug delivery systems for the targeted and controlled release of bioactive substances.

## Acknowledgment

Only if necessary.

## REFERENCES

- [1] Chircov C, Vasile BS. New Approaches in Synthesis and Characterization Methods of Iron Oxide Nanoparticles. In: Xiao-Lan H, editor. Iron Oxide Nanoparticles. Rijeka: IntechOpen; 2022.
  - [2] Creutzburg M, Sellschopp K, Gleißner R, Arndt B, Vonbun-Feldbauer GB, Vonk V, et al., *Surface structure of magnetite (111) under oxidizing and reducing conditions*, Journal of Physics: Condensed Matter, **34**, 164003 (2022).
  - [3] Dheyab MA, Aziz AA, Jameel MS, Noqta OA, Khaniabadi PM, Mehrdel B, *Simple rapid stabilization method through citric acid modification for magnetite nanoparticles*, Sci Rep, **10**, 10793 (2020).
-

- [4] Kozlenko DP, Dubrovinsky LS, Kichanov SE, Lukin EV, Cerantola V, Chumakov AI, et al., *Magnetic and electronic properties of magnetite across the high pressure anomaly*, Scientific Reports, **9**, 4464 (2019).
- [5] Chircov C, Bîrcă AC, Grumezescu AM, Vasile BS, Oprea O, Nicoară AI, et al., *Synthesis of Magnetite Nanoparticles through a Lab-On-Chip Device*, Materials, **14**, 5906 (2021).
- [6] Niculescu A-G, Chircov C, Grumezescu AM, *Magnetite nanoparticles: Synthesis methods – A comparative review*, Methods, **199**, 16-27 (2022).
- [7] Gieré R, *Magnetite in the human body: Biogenic vs. anthropogenic*, Proc Natl Acad Sci U S A, **113**, 11986-7 (2016).
- [8] Perversi G, Cumby J, Pachoud E, Wright JP, Attfield JP, *The Verwey structure of a natural magnetite*, Chemical Communications, **52**, 4864-7 (2016).
- [9] Rincón-López J, Almanza-Arjona YC, Riascos AP, Rojas-Aguirre Y, *Technological evolution of cyclodextrins in the pharmaceutical field*, J Drug Deliv Sci Technol, **61**, 102156 (2021).
- [10] Synytsia A, Sych O, Iatsenko A, Babutina T, Tomila T, Bykov O, et al., *Effect of type and parameters of synthesis on the properties of magnetite nanoparticles*, Applied Nanoscience, **12**, 929 - 37 (2021).
- [11] Cruz IF, Freire C, Araújo JP, Pereira C, Pereira AM. Chapter 3 - Multifunctional Ferrite Nanoparticles: From Current Trends Toward the Future. In: El-Gendy AA, Barandiarán JM, Hadimani RL, editors. Magnetic Nanostructured Materials: Elsevier; 2018. p. 59-116.
- [12] Wu W, Wu Z, Yu T, Jiang C, Kim WS, *Recent progress on magnetic iron oxide nanoparticles: synthesis, surface functional strategies and biomedical applications*, Sci Technol Adv Mater, **16**, 023501 (2015).
- [13] Besenhard MO, LaGrow AP, Hodzic A, Kriechbaum M, Panariello L, Bais G, et al., *Coprecipitation synthesis of stable iron oxide nanoparticles with NaOH: New insights and continuous production via flow chemistry*, Chemical Engineering Journal, **399**, 125740 (2020).
- [14] Rane AV, Kanny K, Abitha VK, Thomas S. Chapter 5 - Methods for Synthesis of Nanoparticles and Fabrication of Nanocomposites. In: Mohan Bhagyaraj S, Oluwafemi OS, Kalarikkal N, Thomas S, editors. Synthesis of Inorganic Nanomaterials: Woodhead Publishing; 2018. p. 121-39.
- [15] Popescu RC, Andronescu E, Vasile BS, *Recent Advances in Magnetite Nanoparticle Functionalization for Nanomedicine*, Nanomaterials (Basel), **9**, (2019).
- [16] Ramadan R, *Preparation, characterization and application of Ni-doped magnetite*, Applied Physics A, **125**, (2019).
- [17] Yang X, Liu L, Zhang M, Tan W, Qiu G, Zheng L, *Improved removal capacity of magnetite for Cr(VI) by electrochemical reduction*, Journal of Hazardous Materials, **374**, 26-34 (2019).
- [18] Efremova MV, Naumenko VA, Spasova M, Garanina AS, Abakumov MA, Blokhina AD, et al., *Magnetite-Gold nanohybrids as ideal all-in-one platforms for theranostics*, Scientific Reports, **8**, 11295 (2018).
-

- [19] Mendonça E, Faria A, Dias S, Aragón F, Mantilla J, Coaquira J, et al., *Effects of silica coating on the magnetic properties of magnetite nanoparticles*, Surfaces and Interfaces, **14**, (2018).
- [20] Khandan A, Ozada N, Saber-Samandari S, Ghadiri Nejad M, *On the mechanical and biological properties of Bredigite-Magnetite (Ca<sub>7</sub>MgSi<sub>4</sub>O<sub>16</sub>-Fe<sub>3</sub>O<sub>4</sub>) nanocomposite scaffolds*, Ceramics International, **44**, 3141-8 (2018).
- [21] Gu H, Zhou X, Lyu S, Pan D, Dong M, Wu S, et al., *Magnetic nanocellulose-magnetite aerogel for easy oil adsorption*, J Colloid Interface Sci, **560**, 849-56 (2020).
- [22] Madaan V, Mohan B, Bhankar V, Ranga R, Kumari P, Singh P, et al., *Metal-Decorated CeO<sub>2</sub> nanomaterials for photocatalytic degradation of organic pollutants*, Inorganic Chemistry Communications, **146**, 110099 (2022).
- [23] Dahiya MS, Tomer VK, Duhan S. 31 - Metal-ferrite nanocomposites for targeted drug delivery. In: Inamuddin, Asiri AM, Mohammad A, editors. Applications of Nanocomposite Materials in Drug Delivery: Woodhead Publishing; 2018. p. 737-60.
- [24] Yang G, Park SJ, *Conventional and Microwave Hydrothermal Synthesis and Application of Functional Materials: A Review*, Materials (Basel), **12**, (2019).
- [25] Morsali A, Hashemi L. Chapter Two - Nanoscale coordination polymers: Preparation, function and application. In: Ruiz-Molina D, van Eldik R, editors. Advances in Inorganic Chemistry. 76: Academic Press; 2020. p. 33-72.
- [26] González CMO, Morales EMC, Tellez AdMN, Quezada TES, Kharissova OV, Méndez-Rojas MA. Chapter 18 - CO<sub>2</sub> capture by MOFs. In: Kharisov B, Kharissova O, editors. Handbook of Greener Synthesis of Nanomaterials and Compounds: Elsevier; 2021. p. 407-48.
- [27] Chircov C, Ștefan R-E, Dolete G, Andrei A, Holban AM, Oprea O-C, et al., *Dextran-Coated Iron Oxide Nanoparticles Loaded with Curcumin for Antimicrobial Therapies*, Pharmaceutics, **14**, 1057 (2022).
- [28] Chircov C, Matei M-F, Neacșu IA, Vasile BS, Oprea O-C, Croitoru A-M, et al., *Iron Oxide-Silica Core-Shell Nanoparticles Functionalized with Essential Oils for Antimicrobial Therapies*, Antibiotics, **10**, 1138 (2021).
- [29] Villegas V, de Leon Ramirez J, Hernández-Guevara E, Sicairos S, Hurtado L, Sánchez B, *Synthesis and characterization of magnetite nanoparticles for photocatalysis of nitrobenzene*, Journal of Saudi Chemical Society, **24**, (2019).
- [30] Peng H, Pearce CI, Huang W, Zhu Z, Rosso KM, Liu J, *Reversible Fe (II) uptake/release by magnetite nanoparticles*, Environmental Science: Nano, **5**, 1545-55 (2018).
- [31] Ramírez-García G, Trapiella-Alfonso L, d'Orlyé F, Varenne A. Chapter 17 - Electrophoretic Methods for Characterizing Nanoparticles and Evaluating Their Bio-interactions for Their Further Use as Diagnostic, Imaging, or Therapeutic Tools. In: Poole CF, editor. Capillary Electromigration Separation Methods: Elsevier; 2018. p. 397-421.
-